This is an open access article published under an ACS AuthorChoice License, which permits copying and redistribution of the article or any adaptations for non-commercial purposes.

ACS OMEGA

http://pubs.acs.org/journal/acsodf

Article

# Shape Transformations of Vesicles Induced by Their Adhesion to Flat Surfaces

Jeel Raval and W. T. Góźdź*

Cite This: *ACS Omega* 2020, 5, 16099−16105

Read Online

ACCESS | Metrics & More | Article Recommendations

**ABSTRACT:** The shape transformations of lipid vesicles induced by the adhesion to a flat surface is investigated. We perform the calculations within the framework of the Helfrich spontaneous curvature model. The calculations were performed for a few values of the reduced volume and the spontaneous curvature. The range of stability for different shapes (oblate, prolate, and stomatocyte) of adhered vesicles is determined. New physical phenomena such as budding induced by the adhesion of vesicles are reported.

Different configurations of adhered vesicles. The dark area shows the membrane attached to the flat surface.

Downloaded via 79.184.167.8 on March 2, 2022 at 21:47:50 (UTC).
See https://pubs.acs.org/sharingguidelines for options on how to legitimately share published articles.

## INTRODUCTION

The adhesion of biological cells and vesicles is highly relevant in understanding interactions between cells. It is also important in biotechnological applications such as material implantation or biosensors. Adhesion may play an important role in drug delivery by small vesicles when they have to be attached to a cell to release its content into the cell. There are many different mechanisms of the adhesion. They may result from attraction of the bilayer to the surface[1,2] or other bilayers[3] or from an interaction of sticker molecules incorporated in the adhering surfaces.[4,5] The amount of the surface area that is in contact because of adhesion may depend on the strength of the interactions or the concentration of the sticker molecules.[6,7] It may also depend on the external force, which brings in contact two vesicles or a vesicle and a solid substrate. In this study, we focus on the shape transformations of lipid vesicles caused by their attachment to a flat solid surface. We do not consider any specific mechanism of adhesion. We consider a general case, which may be realized by different physical mechanisms. We assume that a vesicle is already attached and we are interested in the shape of the vesicles with different amounts of the surface of the vesicle in contact with the flat substrate.

The ensemble that mimics such experimental situations is the one with constant surface area $S$ and volume $V$. Such a physical situation is well described by the elastic energy[8−10] given by

$$\mathcal{F} = \frac{\kappa}{2}\int_S \mathrm{d}S(C_1 + C_2 - C_0)^2 \tag{1}$$

where $\kappa$ is the bending rigidity, $C_1$ and $C_2$ are the principal curvatures, $C_0$ is the spontaneous curvature and the integral (1) is taken over the surface of a closed vesicle. The curvature energy is calculated over the whole surface of the vesicle. We have also assumed that the Gaussian rigidity is the same for the adhered and free membrane. No topology changes are assumed, therefore the integral over the Gaussian curvature contributes a constant value and is omitted in eq 1. In order to mimic the experimental conditions, the constraints of constant surface area $S$ and volume $V$ are imposed.

Vesicle shapes can be well-approximated in numerical calculations by surfaces, which are rotationally symmetric. Therefore, the vesicles can be studied by parameterizing their shape with the angle between the horizontal axis and the line tangent to the shape profile, $\theta(s)$, as a function of the arclength $s$. The radius $r(s)$ and the height $z(s)$ of the shape profile are calculated from $\theta(s)$ according to

$$r(s) = \int_0^s \mathrm{d}s' \cos(\theta(s')) \tag{2}$$

$$z(s) = \int_0^s \mathrm{d}s' \sin(\theta(s')) \tag{3}$$

In order to parameterize a closed shape, the following constraints must be satisfied

$$\theta(0) = 0 \tag{4}$$

$$\theta(L_s) = \pi \tag{5}$$

$$r(L_s) = R \tag{6}$$

**Received:** April 8, 2020
**Accepted:** June 15, 2020
**Published:** June 25, 2020



© 2020 American Chemical Society



https://dx.doi.org/10.1021/acsomega.0c01611
*ACS Omega* 2020, 5, 16099−16105

where $L_s$ is the length of the shape profile. The eq 4 and 5 guarantee that the profile is smooth at the ends and eq 6 accounts for the fact that the vesicle may touch the adhesion surface at a distance $r(L_s)$ from the axis of rotation.

The functional (1) with the shape profile parametrized by $\theta(s)$ is given by[11]

$$\mathcal{F}[\theta(s)] = \frac{\kappa}{2}\left[\pi r(L_s)^2 C_0{}^2 + (2\pi) \int_0^{L_s} \mathrm{d}s r(s)\left(\frac{\mathrm{d}\theta(s)}{\mathrm{d}s} + \frac{\sin(\theta(s))}{r(s)} - C_0\right)^2\right] \quad (7)$$

The functional 7 is minimized numerically. The function describing the shape profile $\theta(s)$ is approximated by the Fourier series, eq 8.

$$\theta(s) = \theta_0 \frac{s}{L_s} + \sum_{i=1}^{N} a_i \sin\left(\frac{\pi}{L_s} i \cdot s\right) \quad (8)$$

where $N$ is the number of Fourier modes, and $a_i$ are the Fourier amplitudes. Large number of the amplitudes, of the order of one hundred, is required in order to accurately parameterize complex shapes. $\theta_0$ is the angle at the point where the membrane touches the adhesion surface, $\theta_0 = \theta(L_s)$. We can define this angle as the contact angle and assume that it is $\theta_0 = \pi$ in order to keep the profile of the vesicle smooth at all points. The value $R = r(L_s)$ defines the contact area, $A$, given by $A = \pi R^2$. Thus, we can define $R$ as an adhesion radius. The functional minimization is replaced by the minimization of the function of many variables.[11] The functional 7 is minimized with respect to the amplitudes $a_i$ and the length of the shape profile $L_s$, under the constraint of constant surface area $S$ and volume $V$, and the adhesion radius $R$ where

$$S = \pi r(L_s)^2 + 2\pi \int_0^{L_s} \mathrm{d}s r(s) \quad (9)$$

$$V = \pi \int_0^{L_s} \mathrm{d}s r^2(s) \sin\theta(s) \quad (10)$$

$$R = \int_0^{L_s} \mathrm{d}s' \cos(\theta(s')) \quad (11)$$

The volume, $V_0$, and the radius, $R_0$, of the sphere having the same surface area, $S$, as the investigated vesicles are chosen as the volume and length units, respectively.[1,12]

$$R_0 = \sqrt{S/4\pi} \quad (12)$$

$$V_0 = \frac{4}{3}\pi R_0{}^3 \quad (13)$$

## RESULTS AND DISCUSSION

The behavior of free vesicles with the spontaneous curvature $C_0 = 0$ has been well-established.[13] It has been shown that three types of vesicle shapes are stable for different values of the reduced volume: stomatocyte for small reduced volume, oblate for intermediate, and prolate for large reduced volume. However, the studies of adhered vesicles are still very scarce despite high importance of such phenomena in biological processes. Here, we perform a detailed analysis of the shape transformations of the vesicles due to their adhesion to a flat surface. We have decided to examine the behavior of vesicles, which have been already studied in a free state.[13] They are all axisymmetric in a free state. In our study, we assume that the part of the vesicle, which is attached to the adhesive surface, is fixed. In experiments, it can be achieved, for example, by sticker molecules. We can also imagine that the vesicle is kept by laser tweezers. We are not investigating the situation where the vesicle can freely move over the adsorbing surface and change its orientation. Under the assumptions that we have made all the shapes presented in the article are stable or metastable. We are convinced that within the assumed parametrization of the vesicle membrane we have found all the solutions. Using more universal parametrization may result in additional solutions. However, in most cases, new parametrization would require new constraints and would result in a new physical situation. We study the stability range, shape transformations, and possible phase transitions of the adhered vesicles. In our calculations, we assume rotational symmetry of the vesicles and that its surface completely adheres to the flat substrate. We do not specify the particular type of the physical interaction of the substrate with the surface. Instead, we assume that because of the interactions of the substrate with the vesicle, a fixed amount of the vesicle surface is completely attached to the flat substrate. It can result, for example, from the attachment of the vesicle membrane to some sticker molecules present on the substrate.

We examine how the shapes and the shape transformations of the vesicles are altered by the adhesion to a flat surface. In the calculations, we assume that different amounts of the vesicle surface at the south pole adhere to the flat surface. This portion of the adhered vesicle membrane is circular because we assume the rotational symmetry of the vesicle shape. The amount of the adhered membrane can be indicated by the radius, $R$, of this circular patch attached to the adhesion surface. We change the radius $R$ from 0 to $R_{max}$ where $R = 0$ corresponds to a free vesicle and $R_{max}$ corresponds to the maximum possible adhesion. Beyond $R_{max}$, a vesicle is ruptured.

In Figure 1, we show four families of shapes obtained for the spontaneous curvature $C_0 = 0$ and the reduced volume, $v = 0.545$, calculated for different values of the adhesion radius $R$. The reduced volume was chosen as $v = 0.545$ because for this value, there exist the solutions for three different types of vesicle shapes.

Thus, three of these families originate from the solutions obtained for free vesicles. They are shown in the second, third, and fourth row of Figure 1. The first shape profile in each row represents the stable solution for the smallest and the last one for the largest value of the adhesion radius $R$. In the middle, the solutions for the intermediate values are presented. For the prolate and stomatocyte branches, the first profiles are plotted for $R = 0$. Thus, they are identical to the free vesicle. For the oblate branch, the first profile is plotted for $R = 0.39$. It has to be recalled that the solution for free vesicles of the oblate branch for the small values of the reduced volume self-intersect or have concave shapes, which makes it impossible to maintain this shape when the vesicle adheres to a flat surface at least when the adhesion radius is small. When the adhesion radius for oblate and stomatocyte vesicles is sufficiently large, we obtain the solutions where the membrane at the south pole and the north pole of the vesicle touches each other. This is reflected in the values of the elastic energy where we observe a cusp in the curve plotted for the elastic energy as a function of the adhesion radius, as shown in the inset of Figure 1e. The


https://dx.doi.org/10.1021/acsomega.0c01611
ACS Omega 2020, 5, 16099−16105

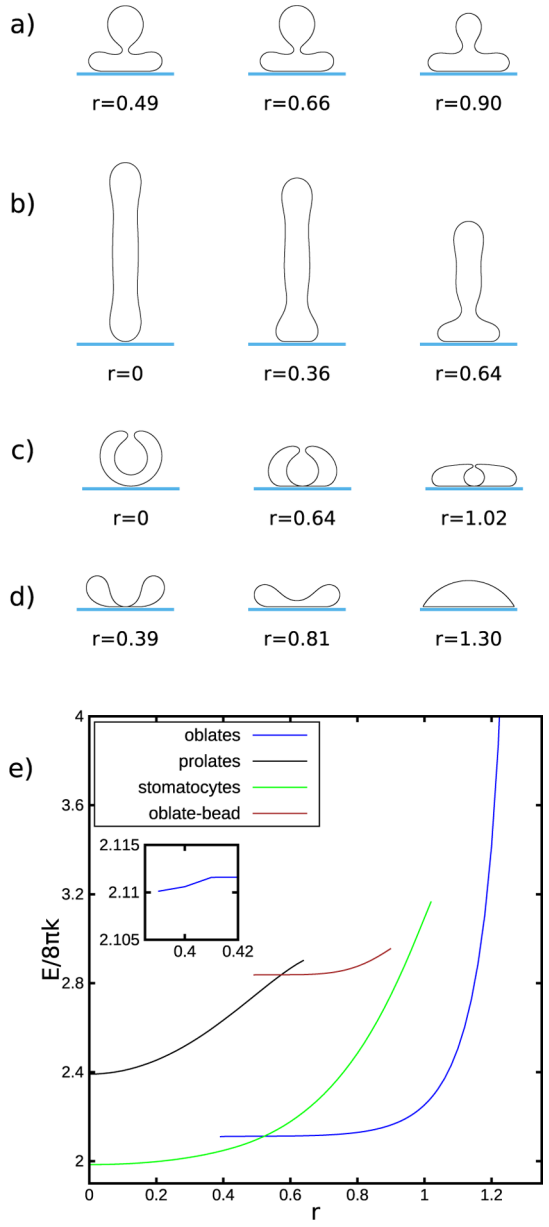


**Figure 1.** Shape profiles for the reduced volume $v$ = 0.545 and spontaneous curvature $C_0$ = 0.0 and different values of the adhesion radius $R=r(L_s)$. (a) New branch of the solutions - oblate-bead, (b) prolate, (c) stomatocyte, (d) oblate branch. (e) Elastic energy, $E/(8\pi\kappa)$, as a function of the adhesion radius, $R$, for different families of solution for the reduced volume $v$ = 0.545 and the spontaneous curvature $C_0$ = 0. The inset shows that the bending energy does not change smoothly when the membrane at the north pole of the vesicle touches the membrane at the south pole.

new family of shapes shown in Figure 1a is stable only in the case of adhered vesicles. Thus, the first stable solution is obtained for the adhesion radius greater than zero.

The plot of the values of the elastic energies as a function of the adhesion radius for all four branches for the full range of stability is shown in Figure 1e. Considering the values of the elastic energy, we can conclude that the most probable configurations for the adhered vesicles with the spontaneous curvature $C_0$ = 0 and the reduced volume $v$ = 0.545 are the configurations, which originated from the stomatocyte branch for the low adhesion radius and oblate vesicle for the large adhesion radius. Because the adhesion radius depends on the strength of the adhesion, we can expect that for the small adhesion strength, we should observe stomatocyte-like configurations (Figure 1c), and for large adhesion strength, we should observe oblate-like configurations (Figure 1d). It is worth to stress that adhesion may induce new transformation of a vesicle, which leads to the shape not observed in the case of free vesicles, as shown in Figure 1a. It is also worth to note that prolate-like (Figure 1b) vesicles are not likely to survive in an adhered state. It can be expected that the vesicles most likely observed in experiments will be oblate ones with large reduced volume and zero spontaneous curvature. We have performed a series of calculations for such vesicles with a few values of the reduced volume to check how much of the vesicle membrane can adhere to the flat surface. We have found that despite large values of the reduced volume, the vesicles can be deformed in such a way that relatively large part of the membrane can adhere to a flat surface. We have calculated that the maximal adhesion radius can be as large as $R$ = 0.70 in the case of the reduced volume $v$ = 0.98, and for $v$ = 0.90 it is as large as $R$ = 0.96. The shape of the nonadhered part of the vesicles is approximately spherical. It is interesting to note that the height of the vesicle increases when larger and larger part of the vesicle membrane is attached to the flat surface. The relation between the height of the vesicle and the adhesion process may be useful in the analysis of experimental results. The changes of the height of a vesicle may indicate potential changes in the strength of the adhesion.

The solutions for oblate and prolate shapes with the spontaneous curvature $C_0$ = 0 have always up-down symmetry. When the spontaneous curvature is sufficiently different from zero, this up-down symmetry is broken and the solutions with pear-like shape are obtained. In such a case, the adhered vesicle may behave in a different way when the smaller or the larger spherical part of the membrane adheres to a flat surface. In Figure 2, we present the calculations performed for the spontaneous curvature, $C_0$ = 2.4, and the reduced volume, $v$ = 0.80.

In the first row (Figure 2a), we present the shape transformation caused by the attachment of the smaller spherical part of the vesicle to the flat surface. It can be noticed that the neck that connects the two spherical parts of the vesicle gets smaller when the adhered surface area of the membrane composing a vesicle gets larger and larger, that is, the adhesion radius is increasing. It has been estimated that $R$ = 0.51 is the limiting adhesion radius for the stability of the vesicle. The limiting shape of the vesicle at $R$ = 0.51 is shown in Figure 2a in the last column. We can speculate that such a behavior may lead to budding of the vesicle because of its adhesion. The vesicle behaves in quite an opposite way when it is attached to the surface from the other end, the larger spherical part. When the adhesion radius is increased, the neck widens until the limiting configuration is obtained for $R$ = 0.61, as shown in Figure 2b. Thus, the vesicles that have a pear shape may behave in a different way when adhered, depending which part of the vesicle is attached to the adhesion surface.

In Figure 2c, we present the shape transformation of a prolate vesicle when the adhesion radius is increased. It is worth noting that the attached prolate vesicles are stable for a wide range of the adhesion radius $0 < R < 0.82$. The second interesting feature of the adhered prolate vesicle is its unique shape, which is different from any free vesicle shape obtained in the spontaneous curvature model (see the most right


https://dx.doi.org/10.1021/acsomega.0c01611
ACS Omega 2020, 5, 16099−16105

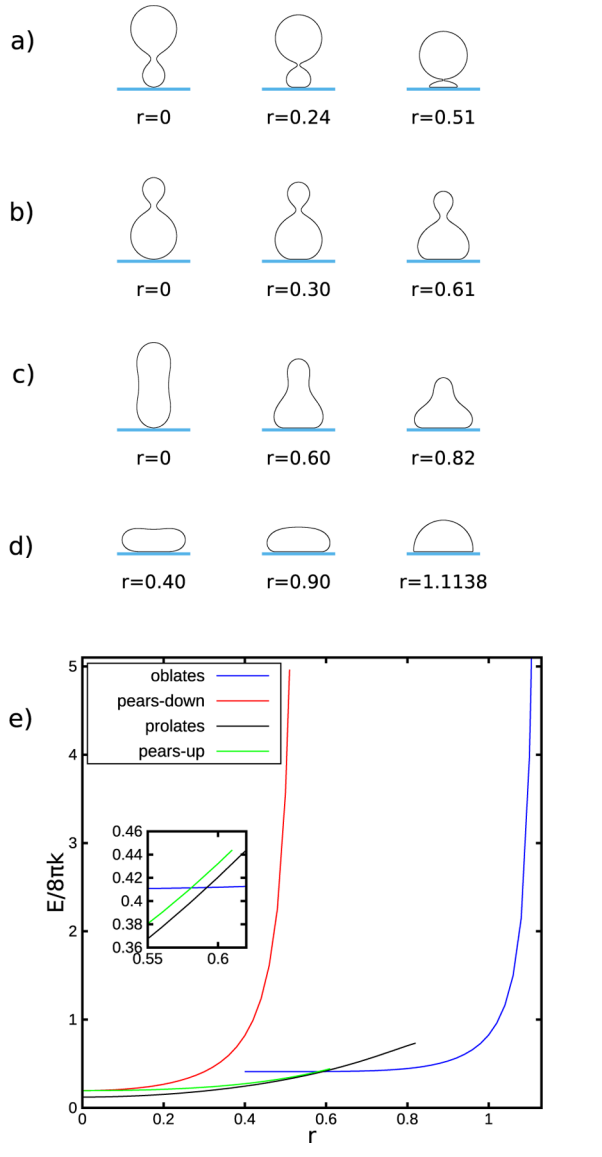


**Figure 2.** Shape profiles for the reduced volume $v$ = 0.8 and spontaneous curvature $C_0$ = 2.4 and different values of the adhesion radius $R=r(L_s)$. The pear branch with the vesicle attached to the surface with smaller (a) and larger (b) bead. The prolate (c) and oblate (d) branch. (e) Elastic energy, $E/(8\pi\kappa)$, as a function of the adhesion radius, $R$, for different families of solution for the reduced volume $v$ = 0.80 and the spontaneous curvature $C_0$ = 2.4. The inset shows the values of the bending energy for different configurations at the intersection.

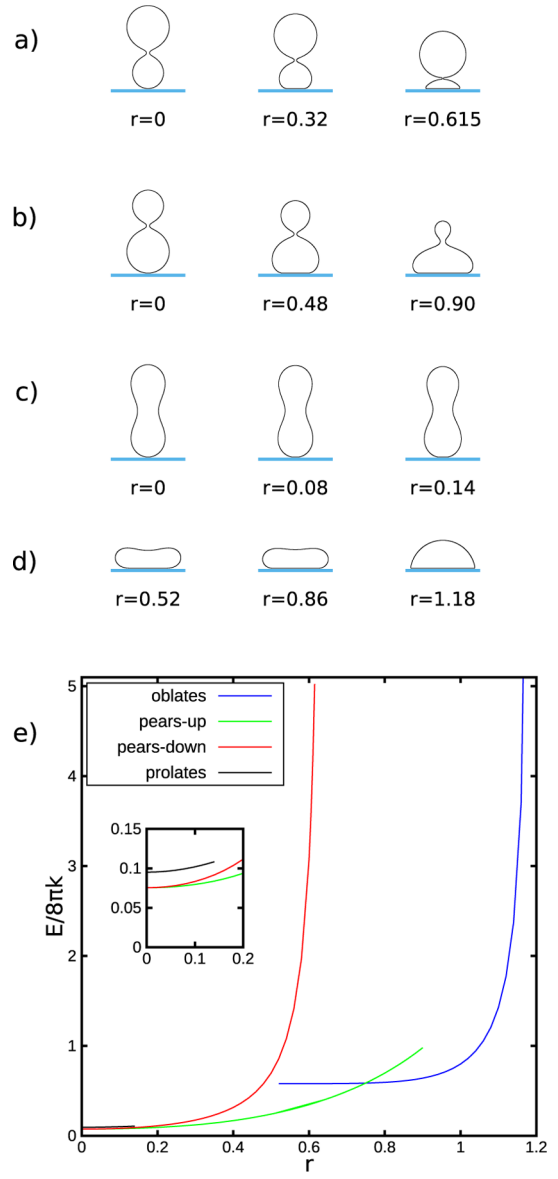


**Figure 3.** Shape profiles for the reduced volume $v$ = 0.7277 and spontaneous curvature $C_0$ = 2.4 and different values of the adhesion radius $R=r(L_s)$. The pear branch with the vesicle attached to the surface with smaller (a) and larger (b) bead. The prolate (c) and the oblate (d) branch. (e) Elastic energy, $E/(8\pi\kappa)$, as a function of the adhesion radius, $R$, for different families of solution for the reduced volume $v$ = 0.7277 and the spontaneous curvature $C_0$ = 2.4. The inset shows the values of the bending energy for small adhesion radii.

configuration in Figure 2c). It can be expected that it will be more probable to change the shape from prolate to oblate for adhered vesicles with such a large reduced volume when the radius of adhesion is high, and indeed this is what we can deduce from the plot of the elastic energy (see Figure 2e). However, it is still surprising that there exist metastable-adhered prolate vesicles for $0.6 < R < 0.82$.

In Figure 3, the possible shape transformation of vesicles for the reduced volume, $v$ = 0.7277, and the spontaneous curvature, $C_0$ = 2.4 are shown. They look similar to the transformations shown in Figure 2, which are performed for the same spontaneous curvature and larger reduced volume. However, there is a significant difference. For smaller reduced volume, the stability range of adhered pear vesicles is increased to as large an adhesion radius as $R$ = 0.9. Surprisingly, the stability range of the prolate vesicle is substantially decreased. We have obtained adhered prolate vesicles only for the adhesion radius in the range $0 < R < 0.14$. For this range of the adhesion radius, the shape of the vesicle does not change significantly. There are no longer even metastable configurations obtained, which are significantly different from the shapes of free vesicles as it was in the case of larger reduced volume. For $v$ = 0.8, the stability range of the pear-like shape was smaller than the stability range of prolate-like vesicles, but for $v$ = 0.7277, it is reversed. We may speculate that budding of the vesicles due to adhesion is more probable for the vesicles with lower reduced volume $v$.



https://dx.doi.org/10.1021/acsomega.0c01611
ACS Omega 2020, 5, 16099−16105

The adhered oblate vesicles are stabilized for the larger adhesion radius, as shown in the elastic energy plot in Figure 3e.

The prolate vesicles are stabilized by a larger spontaneous curvature. Here, we would like to examine how such prolate vesicles behave when attached to the flat surface. The shape profiles calculated for the reduced volume $v = 0.545$ and the spontaneous curvature $C_0 = 3.0$ are shown in Figure 4.

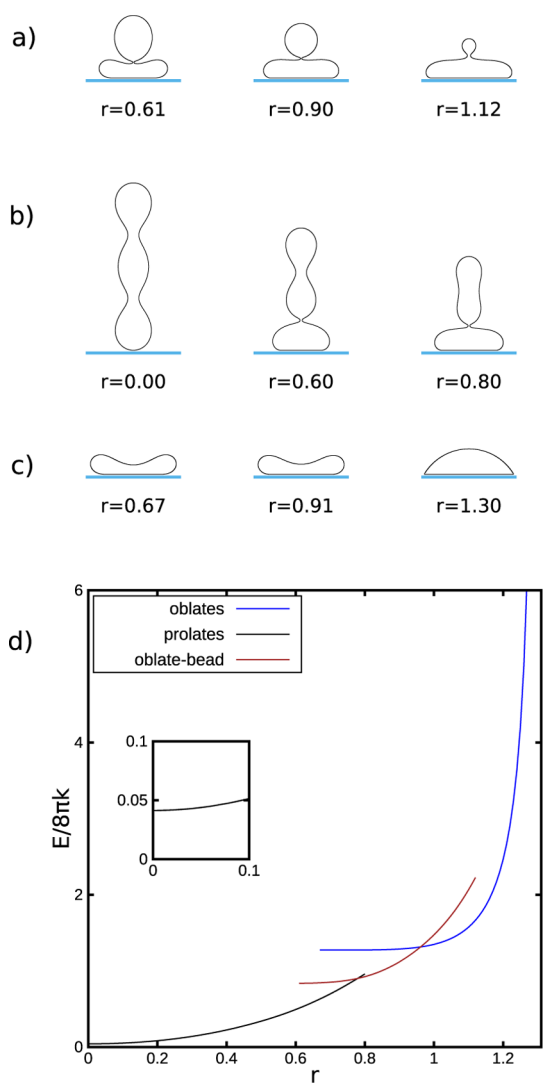


**Figure 4.** Shape profiles for the reduced volume $v = 0.545$ and spontaneous curvature $C_0 = 3.0$ and different values of the adhesion radius $R=r(L_s)$. (a) Oblate with a bead branch, (b) prolate branch, (c) oblate branch. (d) Elastic energy, $E/(8\pi\kappa)$, as a function of the adhesion radius $R=r(L_s)$, for different families of solution for the reduced volume $v = 0.545$ and the spontaneous curvature $C_0 = 3.0$. The inset shows the values of the bending energy for small adhesion radii.

We can see that the range of the adhesion radius for the attached stable prolate vesicle is quite wide $0 < R < 0.8$. For sufficiently large $R$, the vesicle is composed of two parts connected by a small neck. One part attached to the surface has an oblate shape, and the second part forms a prolate-shape bud. It is interesting to note that for the same values of the adhesion radius, two different configurations of vesicles composed of two parts connected by a small neck can exist. In the first configuration, this bud has a spherical shape (Figure 4a), and in the second configuration, this bud has a prolate shape (Figure 4b). The configuration with the spherical bud is more stable for larger values of the adhesion radius, and the configuration with the prolate bud is stable for smaller values of the adhesion radius, as shown in the plot of the elastic energy in Figure 4d. There is a value of the adhesion radius $R$, at which these two configurations with buds have the same elastic energy. It might indicate the possibility of an easy transformation from one configuration to the other. Similarly, at larger value of the adhesion radius, the oblate vesicle (Figure 4c) and the oblate vesicles with a bud (Figure 4a) have the same energy. We can also notice that the spherical bud changes its shape with the increasing adhesion radius $R$. The bud gets smaller and smaller until it disappears approximately at $R = 1.12$. For the largest values of $R$, the only stable configurations are adhered vesicles with the oblate shape (Figure 4c). There is a range of values of the adhesion radius where the stable solutions for all three configurations of adhered vesicles are obtained, as shown in Figure 4d.

In the calculations for $v = 0.545$, we have shown that the increasing adhesion radius $R$ causes the decrease in the size of the spherical bead for the vesicles composed of two parts connected by a small neck. Here, we would like to examine the shape transformations when we start with the free vesicle composed of two equal spherical beads separated by a small neck. Such free vesicles are obtained for the reduced volume $v = 0.705$ and the spontaneous curvature $C_0 = 3.0$. In Figure 5, we present possible transformations of a symmetric prolate and oblate vesicle for $v = 0.705$ and $C_0 = 3.0$. We can see that also in this case, when the adhesion radius $R$ is increasing, the bead that is not attached to the surface stays spherical and gets smaller. The bead that is attached to the surface becomes oblate and gets larger. For sufficiently large $R$, the spherical bead disappears, and the only stable solutions is the adhered oblate vesicle.

We can see from the plot of the elastic energy (Figure 5c) that the adhered prolate vesicles are stable for quite a wide range of the adhesion radius $0 < R < 1.0$. The adhered oblate vesicles are obtained only for larger values of the adhesion radius $0.55 < R < 1.2$.

In the case of pear-shaped adhered vesicles, we have observed so far that the configurations with a larger spherical part attached to the flat surface have wider range of stability. In Figure 6, we present the vesicle shapes for the reduced volume $v = 0.89$ and the spontaneous curvature $C_0 = 3.0$. It is quite surprising that for such choice of parameters, the configurations with the smaller sphere attached to the surface (Figure 6a) have wider range of stability than the configurations with the larger bead attached to the surface (Figure 6b) in the case of pear-shaped vesicles. The latter solutions are stable only up to $R = 0.02$. For larger $R$, adhered prolate vesicles become metastable up to $R = 0.68$ (Figure 6c).

The adhered oblate vesicles are stable for the full range of the adhesion radius $R$, as shown in the plot of the elastic energy in Figure 6e.

## CONCLUSIONS

We have studied the behavior of the vesicles adhered to a flat surface within the framework of the spontaneous curvature model. The calculations were performed for a few values of the spontaneous curvature and the reduced volume. We have identified the stability range of different branches of solutions


https://dx.doi.org/10.1021/acsomega.0c01611
ACS Omega 2020, 5, 16099−16105

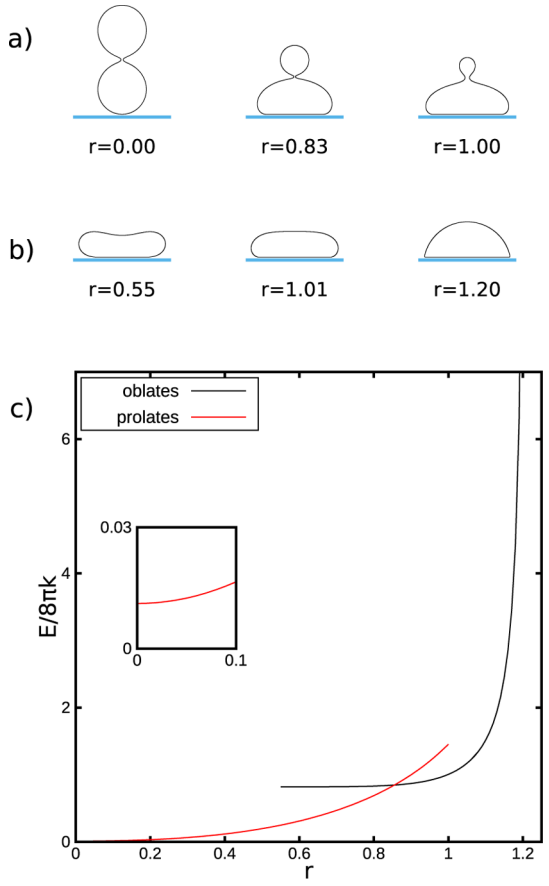


**Figure 5.** Shape profiles for the reduced volume $v$ = 0.705 and the spontaneous curvature $C_0$ = 3.0 and different values of the adhesion radius $R=r(L_s)$. (a) Prolate and (b) oblate branch. (c) Elastic energy, $E/(8\pi\kappa)$, as a function of the adhesion radius, $R$, for different families of solution for the reduced volume $v$ = 0.705 and the spontaneous curvature $C_0$ = 3.0. The inset shows the values of the bending energy for small adhesion radii.

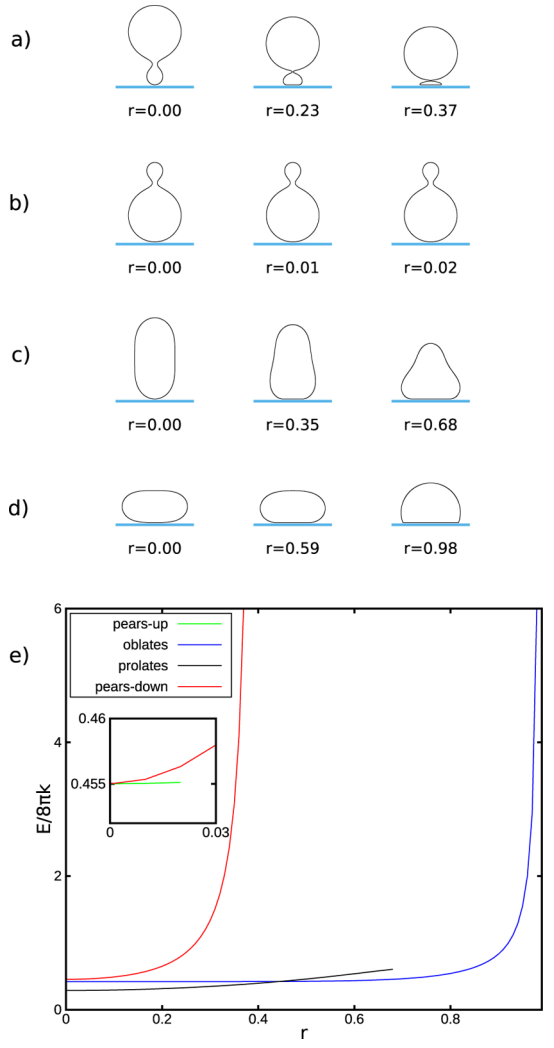


**Figure 6.** Shape profiles for the reduced volume $v$ = 0.89 and the spontaneous curvature $C_0$ = 3.0. The pear branch with the vesicle attached to the surface with smaller (a) and larger (b) bead. The prolate (c) and oblate (d) branch. (e) Elastic energy $E/(8\pi\kappa)$ as a function of the adhesion radius $R=r(L_s)$, for different families of solution for the reduced volume $v$ = 0.89 and the spontaneous curvature $C_0$ = 3.0. The inset shows the values of the bending energy for small adhesion radii.

as a function of the adhesion radius. We have observed the formation of new structures caused by the adhesion of a vesicle to a flat surface. We have discovered that the adhesion of a vesicle may cause the formation of a spherical or a prolate bud connected by a small neck with the vesicle adhered to the flat surface. Such shape transformation may lead to budding, which may be important in biological processes. We have observed that the width of the neck connecting the bud depends on the size of the vesicle patch attached to the surface. Thus, it may be possible to cause budding of the vesicles or biological cells with the change of the adhesion potential. We have obtained in many cases multiple solution with the same energy for the same set of parameters. Such degeneracy may result in interesting phenomena where the adhered vesicle can be transformed from one state to another state of the same energy. It also shows that the unique solution for an adhered vesicle always exists.

The adhesion of a membrane surrounding biological cells is a phenomenon that may be important in many biological processes. Thus, it will be valuable to understand such processes based on the studies performed within relatively simple theoretical models of membranes. We have demonstrated that adhesion may lead to many qualitatively different shape transformations depending on the reduced volume and the spontaneous curvature. We may speculate that such a versatile behavior may be exploited in many biological processes. We hope that the results presented here will help understand the behavior of the biological systems observed in experiments and will help design new experiments.

## AUTHOR INFORMATION

### Corresponding Author

**W. T. Góźdź** − *Institute of Physical Chemistry Polish Academy of Sciences, 01-224 Warsaw, Poland;* orcid.org/0000-0003-4506-6831; Email: wtg@ichf.edu.pl

### Author

**Jeel Raval** − *Institute of Physical Chemistry Polish Academy of Sciences, 01-224 Warsaw, Poland*

Complete contact information is available at: https://pubs.acs.org/10.1021/acsomega.0c01611



https://dx.doi.org/10.1021/acsomega.0c01611
*ACS Omega* 2020, 5, 16099−16105

### Notes

The authors declare no competing financial interest.

## ■ ACKNOWLEDGMENTS

This publication is a part of a project that has received funding from the European Union's Horizon 2020 research and innovation programme under the Marie Skłodowska-Curie grant agreement no. 711859 to J.R. and no. 734276 to H.S, and W.G. Additional funding was received from the Ministry of Science and Higher Education of Poland for the project no. 734276 in the years 2017-2018 (agreement no. 3854/H2020/17/2018/2) and for the implementation of the international cofinanced project no. 711859 in the years 2017-2021. WG would like to acknowledge the support from NCN grant no 2018/30/Q/ST3/00434.

## ■ REFERENCES

(1) Seifert, U.; Lipowsky, R. Adhesion of vesicles. *Phys. Rev. A: At., Mol., Opt. Phys.* **1990**, *42*, 4768−4771.
(2) Seifert, U. Adhesion of vesicles in two dimensions. *Phys. Rev. A: At., Mol., Opt. Phys.* **1991**, *43*, 6803−6814.
(3) Ziherl, P.; Svetina, S. Flat and sigmoidally curved contact zones in vesicle−vesicle adhesion. *Proc. Natl. Acad. Sci. U.S.A.* **2007**, *104*, 761−765.
(4) Bell, G. I.; Dembo, M.; Bongrand, P. Cell adhesion. Competition between nonspecific repulsion and specific bonding. *Biophys. J.* **1984**, *45*, 1051−1064.
(5) Brochard-Wyart, F.; de Gennes, P. G. Adhesion induced by mobile binders: Dynamics. *Proc. Natl. Acad. Sci. U.S.A.* **2002**, *99*, 7854−7859.
(6) Swain, P. S.; Andelman, D. The Influence of Substrate Structure on Membrane Adhesion. *Langmuir* **1999**, *15*, 8902−8914.
(7) Weikl, T. R.; Asfaw, M.; Krobath, H.; Różycki, B.; Lipowsky, R. Adhesion of membranesviareceptor−ligand complexes: Domain formation, binding cooperativity, and active processes. *Soft Matter* **2009**, *5*, 3213−3224.
(8) Helfrich, W. Elastic properties of lipid bilayers: theory and possible experiments. *Z. Naturforsch.* **1973**, *28*, 693−703.
(9) Evans, E. A. Bending resistance and chemically induced moments in membrane bilayers. *Biophys. J.* **1974**, *14*, 923−931.
(10) Canham, P. B. The minimum energy of bending as a possible explanation of the biconcave shape of the human red blood cell. *J. Theor. Biol.* **1970**, *26*, 61−81.
(11) Góźdź, W. T. Spontaneous Curvature Induced Shape Transformations of Tubular Polymersomes. *Langmuir* **2004**, *20*, 7385−7391.
(12) Miao, L.; Fourcade, B.; Rao, M.; Wortis, M.; Zia, R. K. P. Equilibrium budding and vesiculation in the curvature model of fluid lipid vesicles. *Phys. Rev. A: At., Mol., Opt. Phys.* **1991**, *43*, 6843−6856.
(13) Seifert, U.; Berndl, K.; Lipowsky, R. Shape transformations of vesicles: Phase diagram for spontaneous- curvature and bilayer-coupling models. *Phys. Rev. A: At., Mol., Opt. Phys.* **1991**, *44*, 1182−1202.



https://dx.doi.org/10.1021/acsomega.0c01611
*ACS Omega* 2020, 5, 16099−16105